Original Paper

Cellular Physiology and Biochemistry

Cell Physiol Biochem 2010;25:433-442

Accepted: January 08, 2010

Cardiac Electrophysiological and Antiarrhythmic Effects of *N*-n-butyl Haloperidol Iodide

Fen-Fei Gao[1], Si-Yuan Hao[2], Zhan-Qin Huang[1], Yan-Mei Zhang[1], Yan-Qiong Zhou[1], Yi-Cun Chen[1], Xing-Ping Liu[1] and Gang-Gang Shi[1,3]

[1]Department of Pharmacology, [2]Department of Pharmacy, First Affiliated Hospital, [3]Department of Cardiovascular Diseases, First Affiliated Hospital, Shantou University Medical College, Shantou

Key Words

N-n-butyl haloperidol • Arrhythmia • Electrophysiology • Ionic currents • Ventricular myocytes

Abstract

Aims: *N*-n-butyl haloperidol (F_2), a novel compound of quaternary ammonium salt derivatives of haloperidol, was reported to antagonize myocardial ischemia/reperfusion injuries. The antiarrhythmic potential and electrophysiological effects of F_2 on rat cardiac tissues were investigated. Methods and Results: In Langendorff-perfused rat hearts, the ventricular arrhythmias were induced by left anterior descending coronary artery of rat heart ligated for 20 min before the release of the ligature. F_2 provided some inhibitive effects against ischemia- and reperfusion-induced ventricular arrhythmias. In His bundle electrogram and epicardial ECG recordings, the drug produced bradycardia, delayed the conduction through the atrioventricular node and prolonged the Wenckebach cycle length and atrioventricular nodal effective refractory period. In whole-cell patch-clamp study, F_2 primarily inhibited the L-type Ca^{2+} current ($I_{Ca,L}$) (IC_{50} = 0.17 μM) with tonic blocking properties and little use-dependence. And the drug also decreased the Na^+ current (IC_{50} = 77.5 μM), the transient outward K^+ current (IC_{50} = 20.4 μM), the steady-state outward K^+ current (IC_{50} = 56.2 μM) and the inward rectifier K^+ current (IC_{50} = 127.3 μM). Conclusion: F_2 may be a promising drug for the treatment of ischemic heart disease with cardiac arrhythmia.

Introduction

Patients with ischaemic heart disease often experience events of ventricular tachyarrhythmia that may even culminate in sudden cardiac death. However, the CAST investigation [1, 2] found that some class I_c antiarrhythmics significantly increased postinfartction mortality. Moreover, the SWORD study documented that *d*-sotalol, a "pure" class III agent, caused torsade de pointes arrhythmias, and even might increase mortality in subsets of patients with myocardial infarction and lowered ejection fraction [3]. Prevention of ventricular arrhythmias and sudden cardiac death remains a continuing challenge in drug development despite intensive research in recent years.

KARGER

Fax +41 61 306 12 34
E-Mail karger@karger.ch
www.karger.com

1015-8987/10/0255-0433$26.00/0

Accessible online at:
www.karger.com/cpb

Gang-Gang Shi, Ph.D.
Department of Pharmacology
Shantou University Medical College
22 Xinling Road, Shantou, Guangdong 515041 (China)
Tel. +86-754-88900301, Fax +86-754-88557562, E-Mail ggshi@stu.edu.cn

N-n-butyl haloperidol (F_2), a novel compound of quaternary ammonium salt derivatives of haloperidol, was found to maintain the effect of coronary artery relaxation but have no extrapyramidal side reactions like haloperidol [4]. Our previous studies showed that F_2 could antagonize myocardial injury induced by ischemia/reperfusion in rat and rabbit [5, 6], and its cardioprotective mechanism might be associated with the inhibition of Ca^{2+} overload by blocking calcium channels of ventricular myocytes [7] and the suppression early growth response (Egr)-1 gene overexpresssion induced by myocardial ischemia/reperfusion [8]. As we know, myocardial ischemia/reperfusion can give rise to ventricular tachyarrhythmia, and arrhythmia usually got involved with ion-channel dysfunction. Due to the blocking effect of F_2 on myocardial calcium channels, if F_2 possess the anti-arrhythmic effects, the combination of cardioprotective and antiarrhythmic effects of F_2 may be advantaged in treatment of ischaemic heart disease. We have therefore evaluated the potential of F_2 in prevention of ischaemia/reperfusion induced arrhythmias and its electrophysiological and mechanical actions.

Methods and Materials

Animals

Adult Sprague-Dawley rats of either sex (220-300 g) were used in our experiments. The investigation conforms with the *Guide for the Care and Use of Laboratory Animals* published by the US National Institutes of Health (NIH Publication No. 85-23, revised 1996). All experimental protocols were approved by the Laboratory Animal Ethics Committee of our institution (No. 2007101501).

Ischaemia- and reperfusion-induced arrhythmias

Rats were anaesthetized with sodium pentobarbitone (50 $mg \cdot kg^{-1}$, i.p.), were given heparin (250 units, i.p.), and then were killed by cervical dislocation. The heart was rapidly excised and mounted on a Langendorff apparatus and perfused via the aorta with oxygenated normal Tyrode solution (37°C). Perfusion pressure was constant, with equivalent 70 cm H_2O. ECG involved recording from two silver wire electrodes placed on the aorta and the ventricular apex. Electrical signals were continuously monitored and recorded by computer after digitization by use of a biological data acquisition and analysis system (BL-420, TME Technology Co., Chengdu, China) at a sampling frequency of 1 kHz.

Rat hearts (n = 12 per group) were perfused for an initial 5 min with normal Tyrode solution, then the solution was switched in a randomized, blinded fashion to one of 5 solutions modified by the addition of stock solution to contain 0, 0.1, 0.3, 1.0, or 3.0 μM F_2. The 0 μM stock solution contained only dimethylsufoxide (DMSO), a solvent of F_2. After a further 5 min of perfusion, the left anterior descending coronary artery was ligated for 20 min before the release of the ligature. The establishment of ischaemia/reperfusion was ascertained by the amount of coronary effluent [9]. Successful occlusion was confirmed by 30% - 40% reduction in coronary flow as compared with pre-ischaemic values.

In previous experiments we found that F_2 produced sinus bradycardia. To examine the role of bradycardia in modulating the antiarrhythmic actions of F_2, we performed additional studies in paced rat hearts (n = 12 per group). Methods were as for unpaced hearts (above) except that F_2 was investigated at one concentration only (1.0 μM). Hearts were paced at a frequency of 5 Hz with the inner-installed stimulator of the BL-420 recording system with use of the bipolar atrial and ventricular electrodes (twice threshold current, 1 ms pulse width) [10].

Arrhythmias were defined according to the Lambeth Conventions [11]. When one type of arrhythmia converts into another type without an intervening period of sinus rhythm, each type of arrhythmia is recorded as having been present during the period of assessment.

His bundle electrogram (HBE) and epicardial ECG

In the Langendorff-perfused heart model, the self-made bipolar cannula electrodes, combining the functions of Langendorff-perfusion aortic cannula and recording electrodes, were inserted into the aortic root for HBE recording [12]. The HBE and epicardial ECG signals were continuously monitored and recorded in a computer after digitization through a multichannel physiological signal recording system (RM6240BD, Chengdu Instrument Factory, Chengdu, China). High right atrial pacing electrode was placed near the junction of the superior vena cava and right atrium, and ventricular pacing electrode was placed on the pericardium near the right-ventricular apex. A pacing stimulus of 1 ms duration with an intensity of twice the threshold current was delivered to the heart preparation through the bipolar atrial or ventricular electrodes.

The right atrium was paced at a constant rate (4 Hz) that is slightly faster than the spontaneous heart rate. At this constant rate pacing, the intra-atrial conduction time (SA), atrioventricular nodal conduction time (AH), His-Purkinje conduction time (HV) and ventricular repolarization time (VRT) were measured. The 3 following stimulating protocols were introduced for electrophysiological studies [9]. (1) Incremental right atrial pacing was used to determine the Wenckebach cycle length (WCL). The atrial pacing cycle length was decreased (every 5 s) in steps of 10 ms until a stable 1:1 atrioventricular nodal conduction pattern was lost. The cycle length at which a 1:1 atrioventricular conduction just started to fail was defined as the WCL. (2) After a train of 8 stimuli (S_1) of constant-rate atrial pacing, a single premature stimulus (S_2) was introduced. The coupling interval (S_1S_2) between the last S_1 and S_2 was progressively shortened in 10-ms steps after every train of stimuli until S_2 did not evoke an atrial depolarization wave A_2. The following data were obtained: atrial effective refractory period (AERP), the S_1S_2 interval in which the S_2 just started to fail to evoke an atrial depolarization wave A_2; atrioventricular

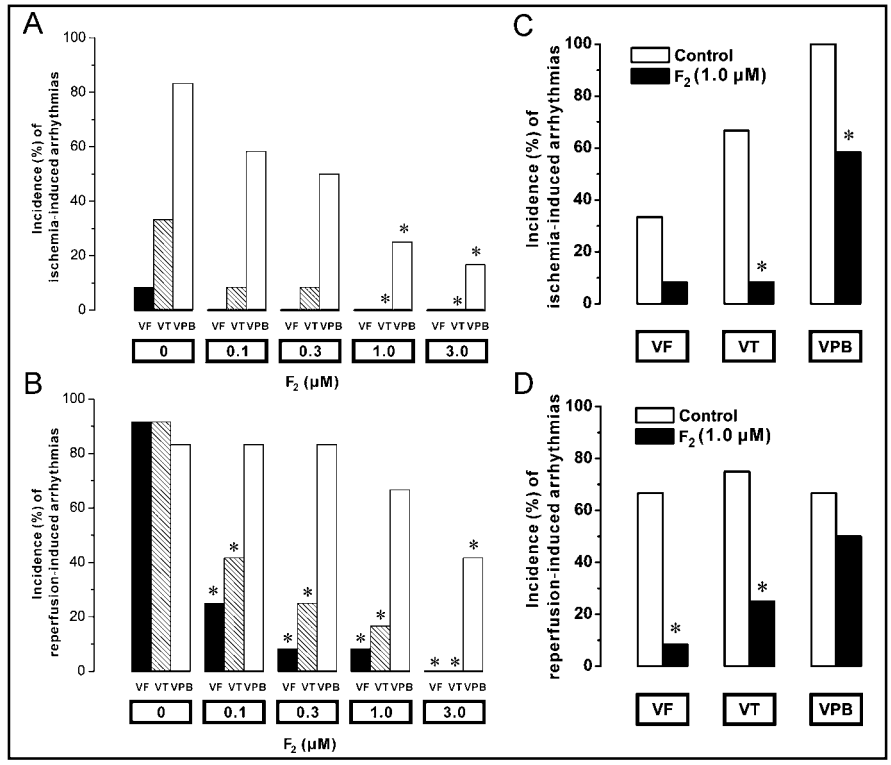

Fig. 1. (A) and (B): Effect of F_2 on group incidences (%) of ischemia- and reperfusion-induced ventricular fibrillation (VF), ventricular tachycardia (VT) and ventricular premature beats (VPB) in rat hearts (n = 12 per group). (C) and (D): Effect of 1 μM F_2 on incidence of ischemia- and reperfusion-induced VF, VT and VPB in rat hearts paced at 5 Hz (n = 12 per group). *P < 0.05 vs control group (0 μM F_2).

nodal effective refractory period (AVNERP), the S_1S_2 interval in which the evoked A_2 just started to fail to evoke a His bundle depolarization wave H_2; and His-Purkinje functional refractory period (HPFRP), the shortest conducted V_1V_2 interval with increasing pacing rate. (3) The ventricular extrastimulation study protocol was similar to protocol one by applying incremental ventricular pacing. The ventricular effective refractory period (VERP) was defined as the pacing cycle length that just started to fail to evoke a premature ventricular depolarization.

The electrophysiological parameters of rat hearts (n = 10) were recorded with initially perfusion of normal Tyrode solution, then recorded after cumulative application of F_2 (0.1-3.0 μM).

Whole-cell patch-clamp recording

Single ventricular myocytes were isolated from the hearts of adult rats by enzymatic dissociation as previously described [7]. Myocytes were perfused with HEPES-buffered Tyrode solution in a recording chamber at room temperature. Membrane potential and currents were recorded by the tight-seal whole-cell configuration with use of an Axopatch 200B amplifier with low-pass filtering at 2 kHz, digitized by DigiData 1322A and processed by pCLAMP 8.2 software (Axon Instruments, Foster City, CA, USA). The electrode capacitance and whole-cell capacitance currents were maximally compensated by use of the amplifier. The series resistance was compensated by 60% to 80%. The liquid junction potential between pipette and bath medium was not corrected.

Solutions and drugs

The normal Tyrode solution contained (in mM): NaCl 137.0, KCl 5.4, $MgCl_2$ 1.0, NaH_2PO_4 0.33, $CaCl_2$ 1.8, glucose 10.0 and $NaHCO_3$ 1.5. The HEPES-buffered Tyrode solution contained (in mM): NaCl 135.0, KCl 5.4, $MgCl_2$ 1.0, NaH_2PO_4 0.33, $CaCl_2$ 1.8, glucose 10.0 and HEPES 10.0, titrated to pH 7.4 with NaOH. The internal pipette filling solution contained (in mM): KCl 140.0, $MgCl_2$ 1.0, Na_2-ATP 2.0, EGTA 10.0, and HEPES 5.0, adjusted to pH 7.2 with KOH. Na^+ current (I_{Na}) was measured in low extracellular sodium ($[Na^+]_o$=10 mM, with NaCl replaced by Choline-Cl) solution to reduce I_{Na} and improve voltage control. To separate ion currents, we chose to add 30 μM Tetrodotoxin (for elimination of I_{Na}) and/or 0.2 mM $CdCl_2$ (for elimination of I_{Ca}) into the bathing solution, and/or to substitute Cs^+ for K^+ in the bathing and pipette solution (for elimination of I_K). F_2 (synthesized by our lab and identified by Shanghai Organic Chemistry Institute of the Chinese Academy of Sciences; purity greater than 98%) was prepared as 0.1 M stock solution in DMSO and diluted to the desired drug concentration with bathing solution before each experiment, with DMSO less than 1% at the highest F_2 concentration used. At this concentration DMSO by itself had no effect on the cells. Tetrodotoxin was purchased from Fisheries Science and Technology Development Company of Hebei Province, China.

Data analysis and statistics

Gaussian distributed variables are expressed as mean ± SEM. Statistical comparison of data was performed using one-way ANOVA followed by Tukey test for individual significant differences or paired Student's t-test where appropriate. Binomially distributed variables were compared by chi-square test with Yates' correction as appropriate. A $P < 0.05$ was considered significantly different. In the patch-clamp study, concentration-response curves were fitted by the Hill equation:

$$I_{drug} / I_{control} = 1 / [1 + (C / IC_{50})^H]$$

where I_{drug} and $I_{control}$ are the current amplitudes in the

Group [F_2 (μM)]	RR (ms)			PR (ms)			QT (ms)		
	I–10	I–1	I+10	I–10	I–1	I+10	I–10	I–1	I+10
0	238±11	260±12	304±16	42±1	44±1	52±2	82±5	95±7	115±11
0.1	251±13	281±18	318±19	46±2	47±2	60±3*	91±9	94±9	114±16
0.3	225±9	274±16	319±17	40±2	46±2	64±4*	81±5	89±5	109±20
1.0	239±11	317±17*	382±24*	42±1	52±2*	71±6*	83±5	105±12	127±19
3.0	246±12	328±21*	408±27*	45±2	58±3*	76±7*	85±6	108±11	136±22

Table 1. Effect of F_2 on RR, PR and QT intervals of epicardium electrocardiography in rat hearts. Values are means ± SEM (n = 12). I-10, I-1 and I+10 refers to 10 min, 1 min before ischemia and 10 min after ischemia, respectively. All hearts of every group at I-10 were perfused with normal Tyrode solution. *$P < 0.05$ *vs* time-matched control group (0 μM F_2).

presence of the drug at concentration C and absence of the drug, respectively; IC_{50} is the concentration for half-maximal block and H is the Hill coefficient. The inactivation curves of the channel current were fitted by the Boltzmann equation:

$$I / I_{max} = 1 / \{1 + \exp[(V_m - V_h) / k]\}$$

where I gives the current amplitude and I_{max} its maximum, V_m the potential of prepulse, V_h the half-maximal inactivation potential, and k the slope factor. The activation curves of the channel current were also fitted by the Boltzmann equation:

$$G / G_{max} = 1 / \{1 + \exp[(V_h - V_m) / k]\}$$

where conductance of channel (G) was calculated from the current-voltage relationship according to the following equation:

$$G = I / (V_m - V_{rev})$$

where V_{rev} is the reversal potential of the current. The curve fitting was performed by use of OriginLab 7.5 (OriginLab Co., Northampton, MA, USA) and Clampfit 8.2 (Axon).

Results

Inhibition of ischaemia- and reperfusion-induced arrhythmias

In the unpaced rat heart, F_2 significantly reduced the incidence of ischemia- and reperfusion-induced arrhythmias in a concentration-dependent manner. At the highest drug concentration, ventricular tachycardia (VT) and ventricular fibrillation (VF) were completely abolished ($P < 0.05$), and ventricular premature beats (VPB) incidence was significantly reduced (Fig. 1A and B). F_2 significantly widened RR and PR intervals before and during ischemia but had no effect on QT intervals (Table 1). F_2 still possessed its antiarrhythmic actions on ischemia- and reperfusion-induced arrhythmias when hearts were paced at 5 Hz (Fig. 1C and D).

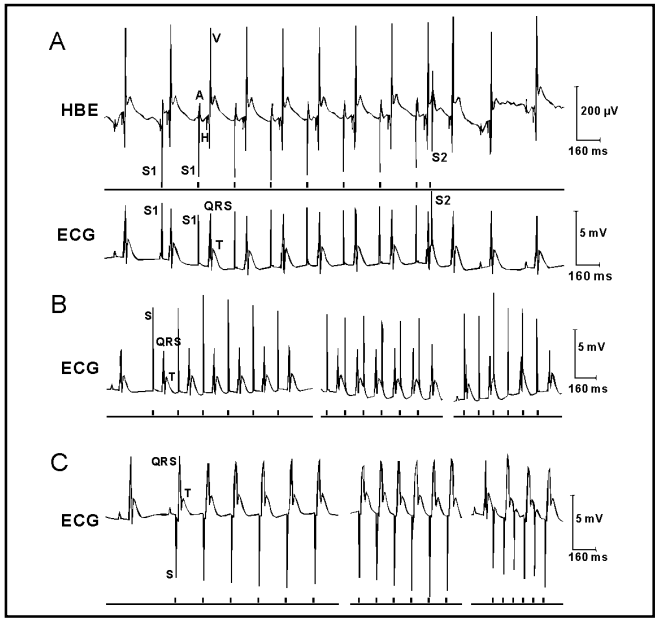

Fig. 2. Representative electrograms for determining the electrophysiological properties of the cardiac conduction system. (A) After a train of 8 stimuli (S_1) of constant rate atrial pacing (4 Hz), a single premature stimulus (S_2) was introduced. The intra-atrial conduction time (SA), AV nodal conduction time (AH), His-Purkinje conduction time (HV) (upper HBE) and ventricular repolarization time (VRT) (lower ECG) were measured. With the coupling interval (S_1S_2) between the last S_1 and S_2 progressively shortened, atrial effective refractory period (AERP), AV nodal effective refractory period (AVNERP), and His-Purkinje functional refractory period (HPFRP) were also measured. (B) Incremental right atrial pacing was used to determine the Wenckebach cycle length (WCL). (C) Incremental ventricular pacing was used to determine the ventricular effective refractory period (VERP). S: stimulation artifact. A: atrial depolarization. H: His bundle depolarization. V: ventricular depolarization. T: ventricular repolarization.

Modification of the electrophysiological properties of the cardiac conduction system

Representative electrograms for determining the electrophysiological properties of the cardiac conduction system are shown in Fig. 2. Changes in the electrophysiological parameters of the cardiac conduction system in 10 rats after cumulative application of F_2 (0.1-3.0 μM) are summarized in Table 2. The conduction interval

F_2 (μM)	SA (ms)	AH (ms)	HV(ms)	VRT (ms)	WCL (ms)	AERP (ms)	AVNERP(ms)	HPFRP (ms)	VERP (ms)
0 (Control)	10 ± 1	40 ± 1	14 ± 1	74 ± 5	129 ± 6	49 ± 2	97 ± 4	130 ± 6	66 ± 3
0.1	10 ± 1	42 ± 2	15 ± 1	76 ± 5	130 ± 7	51 ± 2	108 ± 5	132 ± 3	73 ± 3
0.3	11 ± 1	44 ± 2*	15 ± 2	80 ± 7	143 ± 6*	53 ± 3	120 ± 5*	172 ± 6*	80 ± 3
1.0	10 ± 1	54 ± 4*	17 ± 2	83 ± 4	161 ± 7*	58 ± 3*	150 ± 5*	190 ± 4*	107 ± 4*
3.0	12 ± 1	58 ± 7*	21 ± 2*	90 ± 6*	194 ± 9*	74 ± 4*	178 ± 6*	221 ± 7*	112 ± 7*
Washout	12 ± 1	56 ± 5*	17 ± 2	92 ± 7*	174 ± 10*	59 ± 4*	148 ± 5*	190 ± 4*	103 ± 7*

Table 2. Concentration-related effect of F_2 on the conduction system of rat isolated perfused hearts. Values are means ± SEM (n = 10). SA, sinoatrial conduction interval; AH, atrio-His bundle conduction interval; HV, His-ventricular conduction interval; VRT, ventricular repolarization time interval; WCL, Wenckebach cycle length; AERP, atrial effective refractory period; AVNERP, atrioventricular nodal effective refractory period; HPFRP, His-Purkinje system functional refractory period; VERP, ventricular effective refractory period. *P < 0.05 *vs* control group.

F_2 (μM)	RMP (mV)	APA (mV)	V_{max} (V/s)	APD_{50} (ms)	APD_{90} (ms)
0 (Control)	71.1 ± 0.8	119.0 ± 4.6	136.4 ± 13.7	7.8 ± 0.8	21.1 ± 1.4
0.1	72.2 ± 0.9	121.2 ± 5.5	148.1 ± 16.2	7.2 ± 0.8	20.4 ± 1.5
1	72.9 ± 1.1	116.7 ± 4.5	139.3 ± 16.4	7.2 ± 0.6	19.8 ± 1.0
10	72.6 ± 1.2	103.3 ± 4.5*	125.6 ± 12.5	7.7 ± 0.6	21.5 ± 1.2
100	71.6 ± 1.0	79.8 ± 6.4*	84.4 ± 11.3*	9.4 ± 0.9*	24.1 ± 1.6*
Washout	73.0 ± 1.3	109.5 ± 6.6	130.1 ± 12.8	7.5 ± 0.6	22.0 ± 1.3

Table 3. Effect of F_2 on action potential parameters in rat ventricular myocytes. Values are means ± SEM (n = 6). RMP, resting membrane potential; APA, action potential amplitude; V_{max}, maximum upstroke velocity of depolarization; APD_{50} and APD_{90}, action potential duration measured at 50% and 90% of repolarization, respectively. *P < 0.05 *vs* control group.

through the atrial tissue (SA interval) was not significantly affected. However, the conduction through the atrioventricular node (AH interval) was significantly lengthened by F_2 in a concentration-dependent manner. The conduction through the His-Purkinje system (HV interval) and ventricular repolarization time (VRT) was lengthened by F_2 only at a high concentration (3.0 μM). After 5-min washout of F_2, the lengthened intervals did not recover completely to the interval before treatment. It suggested that F_2 may have high affinity to the myocardial tissues. F_2 concentration-dependently prolonged WCL, AVNERP and HPERP. At high concentrations (1.0, 3.0 μM), AERP and VERP were also prolonged.

Effect of F_2 on action potential

Action potential was elicited in current-clamp mode by 3-ms, 2-nA current injections at 1 Hz. Fig. 3 illustrates the concentration-dependent effects of F_2 on the action potential waveforms in a rat ventricular myocyte. The resting membrane potential was not significantly affected by F_2. At the highest concentration (100 μM), the action potential amplitude (APA) and the maximal upstroke velocity of depolarization (V_{max}) were decreased,

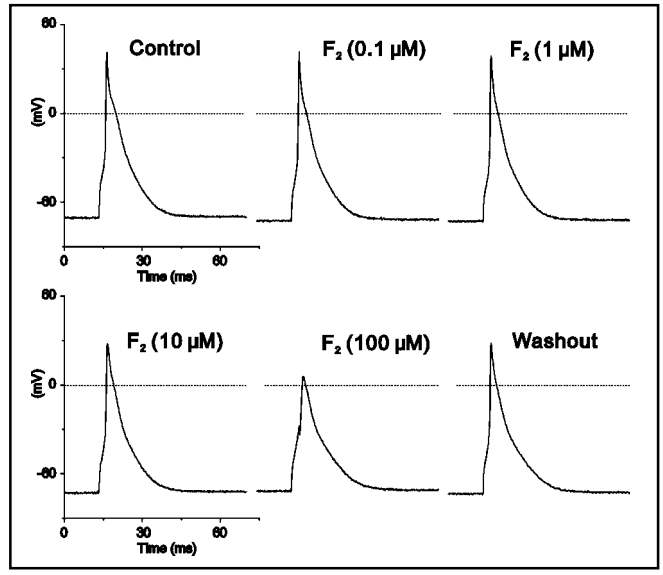

Fig. 3. Effect of F_2 on action potential waveforms in a rat ventricular myocyte.

and the action potential duration at 50% and 90% repolarization (APD_{50} and APD_{90}) was prolonged. The effect of F_2 was reversed after 5-min washout with control solution (Table 3).

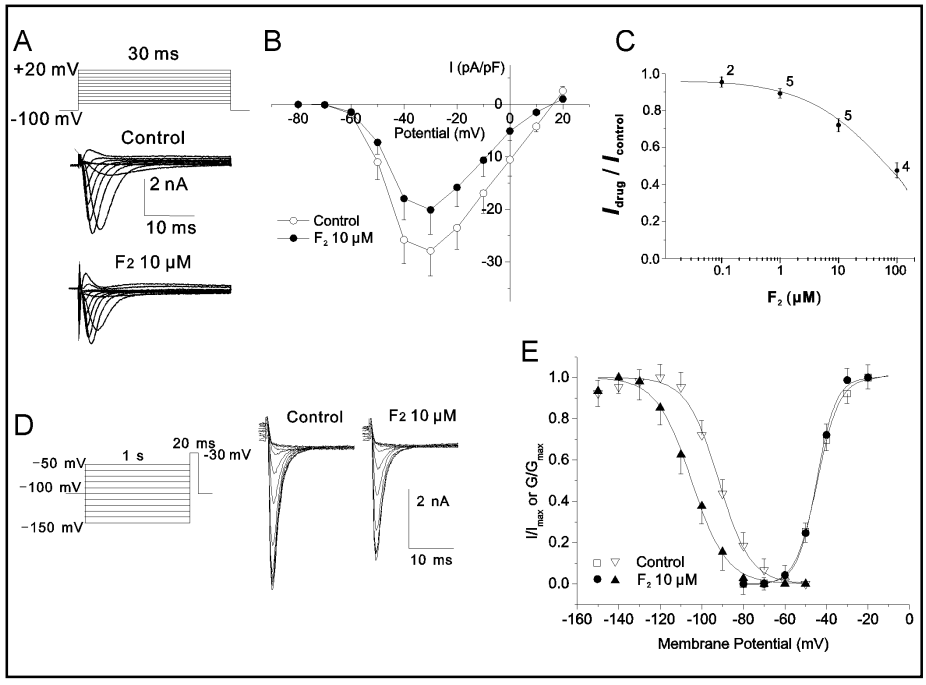

Fig. 4. Effect of F_2 on I_{Na}. (A) The original records of I_{Na} elicited by 30-ms step depolarizations from a holding potential of -100 mV to potentials ranging from -80 to +20 mV under control conditions and after 5-min superfusion with 10 μM F_2. (B) *I-V* relationship for I_{Na}. All currents were normalized for cell capacitance and plotted as mean ± SEM (n=5). (C) Concentration-response curve for the effect of F_2 on I_{Na}. The numbers beside each data point indicate the number of experimental cells. (D) The clamp protocol (left) for voltage-dependent steady-state I_{Na} inactivation and test current traces under control conditions (middle) and after 5-min superfusion with 10 μM F_2 (right). (E) Voltage dependence of steady-state I_{Na} activation and inactivation in the absence and presence of 10 μM F_2.

Effect of F_2 on Na^+ currents (I_{Na})

I_{Na} was elicited by 30 ms step depolarization from a holding potential of -100 mV to potentials ranging from -80 to +20 mV in 10 mV increments at 1 Hz (Fig. 4A). F_2 reduced I_{Na} amplitude at all potentials tested, without changes in either threshold potential or peak potential (Fig. 4B). The concentration-dependent effect of F_2 on I_{Na} at -30 mV was fitted by the Hill equation to revealed a concentration for half-maximal block (IC_{50}) of 77.5 μM and a Hill coefficient (H) of 0.61 (Fig. 4C).

To study the effect of F_2 on the voltage-dependent I_{Na} availability, a double-pulse experiment was applied with a 20 ms test pulse to -30 mV following a 1000 ms conditioning prepulse from the holding potential of -100 mV to potentials ranging from -150 to -50 mV in 10 mV steps (Fig. 4D). The steady-state Na^+ channel inactivation curves were obtained by normalizing I_{Na} amplitudes to their maximum value and were plotted as a function of prepulse membrane potential (Fig. 4E). F_2 appeared to block the Na^+ current by causing a negative shift of the steady-state inactivation curve without affecting the slope factor. On average (n = 3), V_h = -91.9 ± 3.9 mV and k = 7.7 ± 1.8 mV under control conditions, and V_h = -104.9 ± 5.3 mV ($P < 0.05$) and k = 8.4 ± 2.3 mV ($P > 0.05$) with 10 μM F_2. The Na^+ channel activation curves were obtained by normalizing conductance of the Na^+ channel to their maximum value and were plotted as a function of membrane potential (Fig. 4E). F_2 did not affect the voltage dependence for activation.

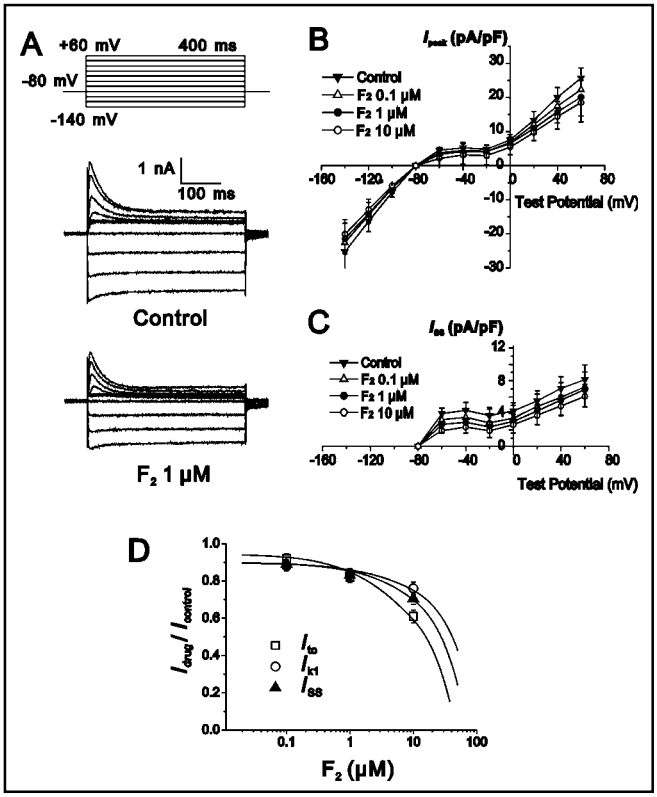

Fig. 5. Effect of F_2 on K^+ currents. (A) Families of current traces elicited by a series of 400-ms long hyperpolarizing or depolarizing pulses ranging from -140 to +60 mV from a holding potential of -80 mV in the absence and presence of 1 μM F_2. (B) and (C) Averaged *I-V* relationship for I_{peak} and I_{SS} observed in the absence and presence of F_2. (D) Concentration-response curve for the effect of F_2 on I_{to}, I_{K1} and I_{SS}.

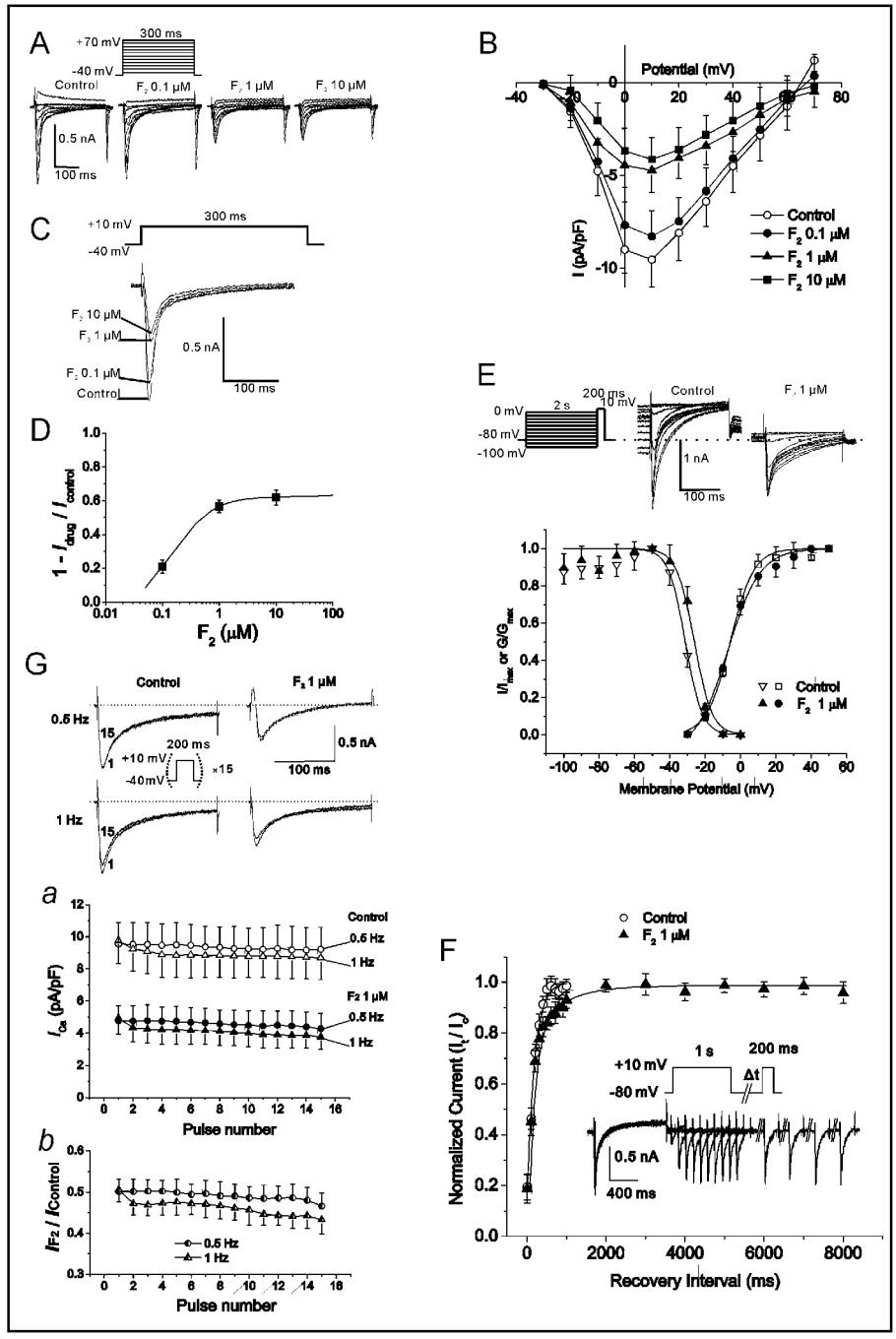

Fig. 6. Effect of F_2 on $I_{Ca\ (L)}$. (A) The original records of $I_{Ca\ (L)}$ elicited by 300-ms step depolarizations from a holding potential of -40 mV to potentials ranging from -30 to +70 mV under control conditions and after superfusion with F_2. (B) *I-V* relationship for $I_{Ca\ (L)}$. (C) The original superimposed records of $I_{Ca,L}$ elicited by 300-ms step depolarization from -40 to +10 mV under control conditions and after superfusion with F_2. (D) Concentration-response curve for the inhibition of F_2 on $I_{Ca,L}$. (E) Effect of F_2 on the voltage dependence of steady-state $I_{Ca,L}$ activation and inactivation. Top: The clamp protocol (left) for voltage-dependent steady-state $I_{Ca,L}$ inactivation and test current traces under control conditions (middle) and after 5-min superfusion with 1 μM F_2 (right). (F) Effects of F_2 on the recovery of $I_{Ca,L}$ from inactivation. $I_{Ca,L}$ completely recovered from inactivation within 500 ms under control conditions. Inset: The double pulse protocol and superimposed records of $I_{Ca,L}$ elicited by the conditioning and test pulse in the presence of 1 μM F_2 (Time axes were broken and the consecutive traces were recorded after 2000-, 3000-, 4000- and 5000-ms recovery interval). (G) Tonic and use-dependent inhibition of $I_{Ca,L}$ by F_2. Superimposed current records of the 1st and 15th $I_{Ca,L}$ obtained on the repetitive depolarizing pulses from -40 to +10 mV at the frequency of 0.5 and 1 Hz during control conditions and after drug superfusion. (Ga) Relation between peak $I_{Ca\ (L)}$ and number of pulses applied at different rates under the control and F_2-application conditions. (Gb) Ratio of peak $I_{Ca,L}$ in presence of F_2 and in control conditions, used as an estimator of the fraction of unblocked channels.

On average (n = 5), V_h = -44.3 ± 3.6 mV and k = 5.2 ± 0.6 mV under control conditions, and V_h = -44.7 ± 4.3 mV and k = 4.7 ± 0.8 mV ($P > 0.05$ for V_h and k) with 10 μM F_2.

Effect of F_2 on K^+ currents

Typical current traces recorded in response to a series of 400 ms hyperpolarizing and depolarizing clamp steps to test potentials between -140 and +60 in 20 mV increments from a holding potential of -80 mV at 0.2 Hz are shown in Fig. 5A. The addition of F_2 (1 μM) to the superfusion solution reduced the amplitude of peak outward K^+ currents (mainly I_{to}) and peak inward K^+ currents through the inward rectifier K^+ channel (mainly I_{K1}). The steady-state K^+ outward currents (I_{SS}) at the end of 400 ms clamp steps were also inhibited. Fig. 5B and C show the current-voltage relation for the peak K^+ currents and I_{SS} before and after the addition of 0.1, 1 and 10 μM F_2. The concentration-dependent effect of F_2 on I_{to} and I_{SS} at +60 mV and on I_{K1} at –140 mV is

shown in Fig. 5D. The IC_{50} values calculated from the concentration-response curve were 20.4, 56.2 and 127.3 μM, and the Hill coefficients were 0.70, 0.72 and 0.63 for I_{to}, I_{SS} and I_{K1}, respectively.

Effect of F_2 on L-type Ca^{2+} current ($I_{Ca,L}$)

To activate $I_{Ca,L}$, we delivered 300 ms pulses to potentials ranging from -30 to +70 mV in 10 mV increments from a holding potential of -40 mV (to inactivate I_{Na} and T-type Ca^{2+} current) at 0.2 Hz. Representative current traces obtained from a ventricular myocyte and the current-voltage relationships in the absence and presence of F_2 are shown in Fig. 6A and B. F_2 reduced $I_{Ca,L}$ amplitude with deceleration of the activation of $I_{Ca,L}$ (Fig. 6C). The activation of currents during a depolarizing pulse (from -40 to +10 mV) was well fitted to mono-exponential function with activation time constants (τ_m) in the absence and presence of F_2. On average (n = 5), the τ_m of $I_{Ca,L}$ was 5.4 ± 1.4 ms during control, and 5.6 ± 1.7 ($P > 0.05$), 10.3 ± 2.6 ($P < 0.05$) and 18.5 ± 4.2 ms ($P < 0.05$) after 0.1, 1 and 10 μM F_2 application, respectively. However, the inactivation of $I_{Ca,L}$ was unaffected. The decay of currents was well fitted by a biexponential function with fast and slow inactivation time constants (τ_f and τ_s). The calculated τ_f and τ_s revealed no significant differences between the absence and presence of F_2. τ_f = 12.7 ± 3.4 ms (control), 13.6 ± 3.8 ms (0.1 μM F_2), 14.0 ± 4.7 ms (1 μM F_2), and 14.5 ± 4.9 ms (10 μM F_2), and τ_s = 126.9 ± 39.4 ms (control), 116.4 ± 37.8 ms (0.1 μM F_2), 144.3 ± 43.1 ms (1 μM F_2), and 153.6 ± 47.4 ms (10 μM F_2). Fig. 6D shows the concentration-dependent curve fitted by the Hill equation with an IC_{50} of 0.17 μM, a Hill coefficient of 1.28 and maximal inhibition E_{max} of 62.4%.

The voltage dependence of steady-state inactivation and activation curves of $I_{Ca,L}$ are shown in Fig. 6E. F_2 (1 μM) caused a small positive-shift of the steady-state inactivation relationship. V_h = –31.2 ± 5.8 mV and k = 4.7 ± 0.9 mV under control, and V_h = –26.2 ± 6.0 mV and k = 5.0 ± 1.1 mV (n = 5, $P > 0.05$ for V_h and k) in the presence of F_2. However, 1 μM F_2 caused an increase of the slope factor of the steady-state activation curve. The values of V_h were -6.3 ± 0.7 mV and -7.2 ± 1.0 mV (n = 5, $P > 0.05$), and the values of k were 6.6 ± 0.6 mV and 9.1 ± 0.9 mV (n = 5, $P < 0.05$) under control and F_2 treatment, respectively.

Recovery of $I_{Ca,L}$ from inactivation was evaluated by a standard double pulse protocol. A 1-s conditioning pre-pulse was applied from -80 to +10 mV to inactivate $I_{Ca,L}$, followed by a 200 ms test-pulse from -80 to +10 mV at intervals (Δt) between 10 ms and 8 s. The frequency of stimulation was 0.1 Hz. The current for each test pulse was normalized to that for the prepulse and plotted as a function of recovery time (Fig. 6F). In control conditions, $I_{Ca,L}$ completely recovered from inactivation within 500 ms, and the time course of recovery from inactivation could be well fitted by a mono-exponential function, with the time constant of recovery τ_{rec} = 190.1 ± 9.1 ms (n = 5). In the presence of 1 μM F_2, recovery of $I_{Ca,L}$ was decelerated and became biexponential, with fast time constant $\tau_{rec,f}$ = 150.6 ± 8.4 ms and slow time constant $\tau_{rec,s}$ = 746.1 ± 11.7 ms (n = 5).

To study the tonic and use-dependent block, a train of 15 depolarizing pulses from -40 to +10 mV for 200 ms was applied at frequencies of 0.5 and 1 Hz. The amplitude of $I_{Ca,L}$ induced by each successive pulse before and after the addition of 1 μM F_2 is plotted in Fig. 6Ga. Tonic blockade was assessed as the difference between the $I_{Ca,L}$ amplitude of the first pulse in the control condition and after drug exposure [13]. In the presence of F_2 (1 μM), the amplitude of $I_{Ca,L}$ evoked by the first pulse in the pulse train was reduced from the control value of 9.54 ± 1.36 pA·pF^{-1} to 4.78 ± 0.94 pA·pF^{-1} (n = 4, $P < 0.05$) at 0.5 Hz and from 9.76 ± 1.41 pA·pF^{-1} to 4.93 ± 0.98 pA·pF^{-1} (n = 4, $P < 0.05$) at 1 Hz. The ratio of $I_{Ca,L}$ in the presence of F_2 to that in control (Fig. 6Gb), which can be used as an approximate parameter of the fraction of unblocked $I_{Ca,L}$ channels [14], did not significantly decrease during the 15 pulses. The ratio of $I_{Ca,L}$ between the first and fifth pulse decreased only by 3.5% (0.5 Hz) and 7.2% (1 Hz). The data suggest that (a) F_2 showed tonic blocking properties and therefore showed some affinity for binding to the resting state of the $I_{Ca,L}$ channel, and (b) inhibition of $I_{Ca,L}$ by F_2 exhibited little use-dependence.

Discussion

The present study examined the potential of F_2 in prophylaxis of ischemia- and reperfusion-induced arrhythmias. The antiarrhythmic action may be mainly mediated through blockade of the Ca^{2+} channels and partly through the Na^+ and K^+ channel. Consequently, F_2 could prolong the atrio-His bundle conduction intervals and the refractoriness of the cardiac conduction system.

An important consequence of both myocardial ischaemia and reperfusion is the occurrence of various

disturbances of cardiac rhythm, including the potential lethal condition of VF [15]. Some anti-ischemic actions can also produce an indirect antiarrhythmogenic action. However, our results showed that F_2 might possess the direct antiarrhythmogenic effect via the influence of cardiac electrophysiology. First, anti-ischemic interventions delay only the onset of ischemia- and reperfusion-induced VF susceptibility [16] but do not suppress arrhythmic rate throughout the time course of ischemia, in contrast to the F_2 findings in the rat (Fig. 1C). Second, pacing rat hearts failed to reverse the protective effects of the drug, as would be expected if anti-ischemic actions contributed to the antiarrhythmic effects [10].

The results showed that F_2 might exert antiarrhythmic activity chiefly via blocking the Ca^{2+} channels. The IC_{50} of F_2 blocking the L-type Ca^{2+} channel was close to its effective antiarrhythmic concentration; however, F_2 had little effect on the Na^+ and K^+ channels at the concentration range used in the present antiarrhythmic study. Drugs that block the L-type Ca^{2+} channel may preferentially slow conduction and increase the refractory period of slow response fibres [17], which are consistent with the observation of PR interval widening and prolongation of AV nodal conduction time, as well as AVNERP and WCL, by F_2 in experiments.

According to the modulated receptor hypothesis, affinity of the drug for the receptor varies with the state of the channel (resting, activated, or inactivated) by the separate rate constants [18, 19]. The results of experiments indicated that F_2 might have higher affinity for binding to the resting state of the L-type Ca^{2+} channel because of its tonic-blocking properties and little use-dependence. The affinity of F_2 to the inactivated- and resting-state Ca^{2+} channels could be estimated by the following equation: $\Delta V_h = k \times \ln[(1 + D/K_R) / (1 + D/K_I)]$ [20], where the ΔV_h is the shift in the midpoint of the steady-state inactivation curve, k is the slope factor, D is the drug concentration, and K_R and K_I are the dissociation constants for resting and inactivated Ca^{2+} channels, respectively. The positive shift of V_h and k produced by 1 μM F_2 (Fig. 6E), along with the value for K_R from Fig. 6D, gives a value of $K_I = 0.70$ μM for binding to the inactivated Ca^{2+} channels, which is slightly greater than K_R (0.17 μM). The deceleration of activation of $I_{Ca,L}$ and no influence on the inactivation of $I_{Ca,L}$ also showed that F_2 could interact with the resting Ca^{2+} channel and had low affinity for binding to the open state. In this study, the recovery process was slowed by F_2 being better described by a double exponential, the slower phase possibly indicating a slow dissociation of drug molecules from the inactivated Ca^{2+} channels [20, 21]. This finding is consistent with F_2 possessing some affinity for binding to the inactivated Ca^{2+} channels. Our results are different from that of Huang, et al. [7], who found that F_2 had a high affinity to the inactivated Ca^{2+} channels from F_2 inducing a negative shift of steady-state inactivation curve and slowing down the recovery from inactivation of $I_{Ca,L}$. The discrepancy with our results could be attributed to the different clamp protocol used and no compensation for capacity or leaky currents in the authors' experiments.

Although F_2 had lower potency in blocking the Na^+ and K^+ channels than the L-type Ca^{2+} channel, it might contribute to synergistic effects on ischemia and reperfusion tachyarrhythmias. F_2 may exert some antiarrhythmic activity by suppression of oscillatory afterpotentials or extrasystole via blocking Na^+ channels and by prolongation of APD and effective refractory period (ERP) via blocking K^+ channels. An $I_{Ca,L}$ blocker will lead to APD_{50} shortening due to a decline of the plateau phase [22]. However, the present study showed that APD_{50} and APD_{90} were not significantly affected by F_2, even prolonged at the highest concentration (100 μM). These results may be related to the inhibition of I_K. Penkoske [23] thought that the cardiac electrophysiology of reperfusion arrhythmia was characterized by refractory period shortening. A pure $I_{Ca,L}$ blocker will aggravate this tendency; however, it can counter-balance the contradiction by the simultaneous inhibition of I_K. Acquired malignant arrhythmia is often involved in multi-channel changes. Under these conditions, blockade of multi-channels may be more useful than inhibition of a single type of ion channel [24].

There is a potential limitation in this study. The effects on ionic current were obtained at room temperature and the kinetics of F_2 block and unblock may be substantially different at physiological temperature.

In conclusion, F_2, a novel compound of a quaternary ammonium salt derivative of haloperidol, exerts class IV antiarrhythmic properties, as well as some blocking K^+ and Na^+ channel effects. F_2 has a chemical structure different from other typical Ca^{2+} channel blockers, yet produces strong effects both on cardiac and coronary artery tissues. The combination of cardioprotective and antiarrhythmic effects suggests that F_2 may be a promising drug for the treatment of ischemic heart disease with cardiac arrhythmia.

Acknowledgements

This work was supported by NSFC-Guangdong Joint Funds (No. U0932005), the Specialized Research Fund for the Doctoral Program of Higher Education of China (No. 200805600003), the National Natural Science Foundation of China (No. 30672465), the Key Project (No. 06118928) and Free Application Project (No. 07008206) of Natural Science Foundation of Guangdong Province of China, the Medical Scientific Research Foundation of Guangdong Province of China (No. A2008435).

References

1 The Cardiac Arrhythmia Suppression Trial (CAST) Investigators: Preliminary report: effect of encainide and flecainide on mortality in a randomized trial of arrhythmia suppression after myocardial infarction. N Engl J Med 1989;321:406-412.

2 The Cardiac Arrhythmia Suppression Trial II Investigators: Effect of the antiarrhythmic agent moricizine on survival after myocardial infarction. N Engl J Med 1992;327:227-233.

3 Waldo AL, Camm AJ, deRuyter H, Friedman PL, MacNeil DJ, Pauls JF, Pitt B, Pratt CM, Schwartz PJ, Veltri EP: Effect of d-sotalol on mortality in patients with left ventricular dysfunction after recent and remote myocardial infarction. The SWORD Investigators. Survival With Oral d-Sotalol. Lancet 1996;348:7-12.

4 Shi GG, Zheng JH, Li CC, Chen JX, Zhuang XX, Chen SG, Liu XP: The effect of quaternary ammonium salt derivation of haloperidol on coromary artery. Chin Pharm J 1998;33:529-531 (Chinese).

5 Huang ZQ, Shi GG, Zheng JH, Liu B: Effects of N-n-butyl haloperidol iodide on rat myocardial ischemia and reperfusion injury and L-type calcium current. Acta Pharmacol Sin 2003;24:757-763.

6 Gao FF, Shi GG, Zheng JH, Liu B: Protective effects of N-n-butyl haloperidol iodide on myocardial ischemia-reperfusion injury in rabbits. Chin J Physiol 2004;47:61-66.

7 Huang ZQ, Shi GG, Gao FF, Zhang YM, Liu XP, Christopher TA, Lopez B, Ma XL: Effects of N-n-butyl haloperidol iodide on L-type calcium channels and intracellular free calcium in rat ventricular myocytes. Biochem Cell Biol 2007;85:182-188.

8 Zhang Y, Shi G, Zheng J, Tang Z, Gao P, Lv Y, Guo F, Jia Q: The protective effects of N-n-butyl haloperidol iodide on myocardial ischemia-reperfusion injury in rats by inhibiting Egr-1 overexpression. Cell Physiol Biochem 2007;20:639-648.

9 Chang GJ, Su MJ, Hung LM, Lee SS: Cardiac electrophysiologic and antiarrhythmic actions of a pavine alkaloid derivative, O-methyl-neocaryachine, in rat heart. Br J Pharmacol 2002;136:459-471.

10 Rees SA, Curtis MJ: Specific IK1 blockade: a new antiarrhythmic mechanism? Effect of RP58866 on ventricular arrhythmias in rat, rabbit, and primate. Circulation 1993;87:1979-1989.

11 Walker MJ, Curtis MJ, Hearse DJ, Campbell RW, Janse MJ, Yellon DM, Cobbe SM, Coker SJ, Harness JB, Harron DW, et al.: The Lambeth Conventions: guidelines for the study of arrhythmias in ischaemia infarction, and reperfusion. Cardiovasc Res 1988;22:447-455.

12 Gao FF, Shi GG, Zhou YQ, Liu XP: Reformative cannula electrodes for His bundle electrogram recording in isolated rat hearts. Chin J Physiol 2008;51:116-119.

13 Delgado C, Tamargo J, Henzel D, Lorente P: Effects of propafenone on calcium current in guinea-pig ventricular myocytes. Br J Pharmacol 1993;108:721-727.

14 Bebarova M, Matejovic P, Pasek M, Novakova M: Effect of haloperidol on transient outward potassium current in rat ventricular myocytes. Eur J Pharmacol 2006;550:15-23.

15 Corr PB, Witkowski FX: Potential electrophysiologic mechanisms responsible for dysrhythmias associated with reperfusion of ischemic myocardium. Circulation 1983;68:I16-24.

16 Bernier M, Curtis MJ, Hearse DJ: Ischemia-induced and reperfusion-induced arrhythmias: importance of heart rate. Am J Physiol 1989;256:H21-31.

17 Harrison DC: Antiarrhythmic drug classification: new science and practical applications. Am J Cardiol 1985;56:185-187.

18 Hondeghem LM, Katzung BG: Time- and voltage-dependent interactions of antiarrhythmic drugs with cardiac sodium channels. Biochim Biophys Acta 1977;472:373-398.

19 Hille B: Local anesthetics: hydrophilic and hydrophobic pathways for the drug-receptor reaction. J Gen Physiol 1977;69:497-515.

20 Bean BP, Cohen CJ, Tsien RW: Lidocaine block of cardiac sodium channels. J Gen Physiol 1983;81:613-642.

21 Hondeghem LM, Katzung BG: Antiarrhythmic agents: the modulated receptor mechanism of action of sodium and calcium channel-blocking drugs. Annu Rev Pharmacol Toxicol 1984;24:387-423.

22 Yatani A, Brown AM, Schwartz A: Bepridil block of cardiac calcium and sodium channels. J Pharmacol Exp Ther 1986;237:9-17.

23 Penkoske PA, Sobel BE, Corr PB: Disparate electrophysiological alterations accompanying dysrhythmia due to coronary occlusion and reperfusion in the cat. Circulation 1978;58:1023-1035.

24 Yong SL, Xu R, McLarnon JG, Zolotoy AB, Beatch GN, Walker MJ: RSD1000: a novel antiarrhythmic agent with increased potency under acidic and high-potassium conditions. J Pharmacol Exp Ther 1999;289:236-244.